Study of Biodegradable Polylactide/Poly(butylene adipate-*co*-terephthalate) Blends

Long Jiang, Michael P. Wolcott, and Jinwen Zhang*

Wood Materials and Engineering Laboratory, Washington State University, Pullman, Washington 99164

Received August 15, 2005; Revised Manuscript Received October 26, 2005

Both polylactide (PLA) and poly(butylene adipate-*co*-terephthalate) (PBAT) are biodegradable polymers. They are thermoplastics which can be processed using most conventional polymer processing methods. PLA is high in strength and modulus (63 MPa and 3.4 GPa, respectively) but brittle (strain at break 3.8%) while PBAT is flexible and tough (strain at break ∼710%). In view of their complementary properties, blending PLA with PBAT becomes a natural choice to improve PLA properties without compromising its biodegradability. In this study, PLA and PBAT were melt blended using a twin screw extruder. Melt elasticity and viscosity of the blends increased with the concentration of PBAT. Crystallization of the PLA component, phase morphology of the blend, mechanical properties, and toughening mechanism were investigated. The blend comprised an immiscible, two-phase system with the PBAT evenly dispersed in the form of ∼300 nm domains within the PLA matrix. The PBAT component accelerated the crystallization rate of PLA but had little effect on its final degree of crystallinity. With the increase in PBAT content (5−20 wt %), the blend showed decreased tensile strength and modulus; however, elongation and toughness were dramatically increased. With the addition of PBAT, the failure mode changed from brittle fracture of the neat PLA to ductile fracture of the blend as demonstrated by tensile test and scanning electron microcopy (SEM) micrographs. Debonding between the PLA and PBAT domains induced large plastic deformation in PLA matrix ligaments.

Introduction

PLA is a linear aliphatic polyester synthesized by ring-opening polymerization of lactides which are the cyclic dimers of lactic acids and are typically derived from corn starch fermentation. PLA has been found to be environmentally biodegradable through a two-step process[1] that begins with the high molecular weight polyester chains hydrolyzing to lower molecular weight oligomers under an appropriate temperature and moisture environment. In the second step, microorganisms convert these lower molecular weight components to carbon dioxide, water, and humus.

Standard-grade PLA has high modulus (3 GPa) and strength (50−70 MPa) comparable to that of many petroleum-based plastics, but its low toughness and physical aging present problems for its applications in medical devices and consumer products. The brittleness of PLA can be modified by copolymerization of lactides with other monomers such as ϵ-caprolactone.[2−4] Hiljanen-Vainio et al. showed that *rac*-PLA copolymer containing 1% caproyl units was hard and brittle. Increasing the caproyl units by a few percent decreased the modulus but substantially increased the elongation.[5] Poly(LLA-*co*-caprolactone) polymerized at higher temperature (110 °C) showed higher elongation than that synthesized at 80 °C because high temperature resulted in a more random structure of the copolymer. The modulus and tensile strength of PLA can be reduced by a factor of 2 after copolymerizing with 10% trimethylene carbonate (TMC).[6] Fifty percent of TMC caused the elongation of the copolymer to increase from 4% to 900% while the tensile strength decreased 10-fold to 5 MPa. Nakayama et al. synthesized a biodegradable polyester by ring-opening copolymerization of L-lactide (LA) with DL-β-methyl-δ-valerolactone (MV).[7] The copolymers containing more than 90 mol % LA formed tough and hard films, whereas those with less than 80 mol % LA formed flexible films similar to natural rubber. Linear and star-shaped copolymers of trimethylene carbonate/ϵ-caprolactone (TMC-*co*-CL) were synthesized and used as a macroinitiator for the subsequent lactide/glycolide polymerization.[8] The resultant copolymer showed extensive toughening effect at relatively low TMC-*co*-CL content. Lactic acid based poly(ester-urethane)s (PEU) were also synthesized by reacting polycondensated PLA prepolymer with diisocyanate.[9−11]

Because none of the aforementioned PLA copolymers are commercially available at this time, blending PLA with other polymers presents a more practical and economic measure to obtain products with properties not currently attainable. Blending PLA with other polymers can substantially modify the mechanical and thermal properties, degradation rate, and permeability. PLA/poly(ϵ-caprolactone) (PCL) blends have been extensively studied.[12−16] Various compatibilizers such as P(LA-*co*-CL) copolymer were used to improve the miscibility between PLA and PCL.[12,14,15,17] The blends displayed good dispersion of the PCL minor phase in the PLA matrix, resulting in better mechanical properties compared to those of neat PLA. Experiments found that the addition of the compatibilizers led to a highly homogeneous structure, while phase separation occurred in the absence of compatibilizers. In the PEU/poly(L-lactic acid-*co*-ϵ-caprolactone-urethane) blend, poly(L-lactic acid-*co*-ϵ-caprolactone-urethane) increased the impact strength of the blend.[18−20] Particulate or fibrous fillers such as wollastonite, kaolinite, and wood fiber added as a third component increased the stiffness.[19] Blends of different stereoisomeric PLAs have also been studied. Mechanical properties and melting temperature were found to be increased due to the formation of stereocomplex crystallites which acted as intermolecular links. On the contrary, nonblended PLA had larger-sized spherulites

* To whom correspondence should be addressed. Phone: 509-335-8723. Fax: 509-335-5077. E-mail: jwzhang@wsu.edu.

10.1021/bm050581q CCC: $33.50
Published on Web 11/23/2005

of less contacting area with the surrounding spherulites.[21−27] PLA was also blended with other nonbiodegradable polymers, including polyethylene, poly(ethylene oxide), poly(ethylene glycol), poly(vinyl acetate), poly(4-vinylphenol), and polyacrylates.[28−34] Varying degrees of property modifications of PLA were achieved by blending with these polymers. Many of these blends are immiscible or only partially miscible and may need compatibilizers to increase their compatibility.

PBAT is an aliphatic−aromatic copolyester, which is fully biodegradable.[35] It degrades within a few weeks with the aid of naturally occurring enzymes. The PBAT supplied by BASF under the trademark of Ecoflex is a flexible plastic designed for film extrusion and extrusion coating. In view of its high toughness and biodegradability, Ecoflex was considered a good candidate for the toughening of PLA. Our overall goal is to produce blends of PLA and PBAT with increased toughness while maintaining biodegradability. The specific objectives of this research are to assess the miscibility, phase morphology, rheology, and mechanical properties of the polymer blend.

Materials and Methods

Polymers. The commercial PLA (Natureworks PLA 4032D, Natureworks) exhibits a density of 1.25 g/cm^3, a weight-average molecular weight of 207 kDa, polydispersity of 1.74 (GPC analysis), and a glass transition temperature and melting point of 66 and 160 °C (differential scanning calorimeter (DSC) analysis), respectively. The PBAT (Ecoflex F BX 7011, BASF Corp.) with density of 1.26 g/cm^3 exhibits a weight-average molecular weight of 145 kDa, polydispersity of 2.40 (GPC analysis), and a glass transition temperature and melting point of −29 and 115 °C (dynamic mechanical analysis (DMA) and DSC analysis), respectively. Both polymers were supplied in pellet form and used as received.

Sample Preparation and Testing. A corotating twin screw extruder (Leistritz ZSE-18) equipped with a volumetric feeder and a strand pelletizer was employed to blend PLA and PBAT. A screw diameter of 17.8 mm and an L/D ratio of 40 were employed. Before extrusion, both the PLA and PBAT pellets were dried in an oven at 60 °C for 8 h. The two polymers were weighed, manually tumbled to premix the pellets, and subsequently fed into the extruder for melt blending. The extrusion temperature was independently controlled on eight zones along the extruder barrel and a strand die to achieve a temperature profile ranging from 150 to 180 °C. The screw speed was maintained at 60 rpm for all runs. After exiting the die, the extrudate was cooled in a water bath before being granulated by a pelletizer. The specific PLA/PBAT blends studied contained 5, 10, 15, and 20 wt % PBAT.

The thermal properties of PLA, PBAT, and their blends were studied by dynamic mechanical analysis (DMA) (Rheometrics solids analyzer, RSAII) and differential scanning calorimetry (Mettler Toledo, DSC 822e). The samples used for DMA analysis were prepared by hot-pressing pellets at 170 °C into a 2 mm thick sheet, which was subsequently air cooled. Specimens ($4 \times 2 \times 45$ mm^3) were cut from the sheet and vibrated in dual-cantilever mode at a frequency of 1 Hz. Prior to analysis, the linear viscoelastic region was determined using a strain sweep. All subsequent tests were conducted at a strain of 0.02% using a 2 °C/min temperature ramp from −60 to 100 °C.

DSC analysis was conducted using specimens sliced from injection-molded material. The specimens were crimp sealed in 40 μL aluminum crucibles. All specimens were heated to 180 °C at 30 °C/min and kept isothermal for 2 min to erase previous thermal history. Then they were cooled to 30 °C at 30 °C/min and subsequently scanned between 30 and 180 °C using two heating rates: 5 and 10 °C/min. The cold crystallization morphology of PLA and PLA/PBAT blends were studied using a polarized optical microscope (Olympus BX51) equipped with a hot stage (Linklam TMS 94). The same temperature ramps were used as in DSC testing.

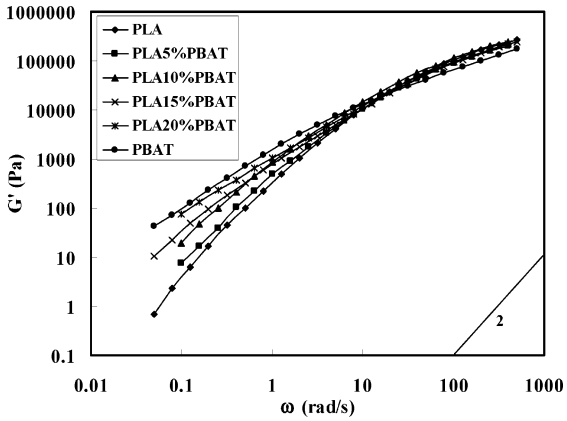

Figure 1. G' of PLA/PBAT blends.

Standard tensile (ASTM D638, type III) and Izod impact (ASTM D256) test samples were prepared by injection molding (Sumitomo SE 50D) operated with a nozzle temperature of 210 °C. Prior to injection molding, the pellets prepared from the blended polymers were dried in an oven at 60 °C for 8 h. Tensile testing was performed on an 8.9 kN, screw-driven universal testing machine (Instron 4466) equipped with a 10 kN electronic load cell and mechanical grips. The tests were conducted at a crosshead speed of 5 mm/min with deflections measured using a 25 mm extensiometer (MTS 634.12E-24) and data acquired by computer. Izod impact test was performed using a standard impact tester (TMI 43-1). All tests were carried out according to the ASTM standard, and five replicates were tested for each sample to get an average value.

Fracture surfaces from the impact and tensile tests were examined using scanning electron microscopy (SEM) (Hitachi S-570). All specimens were sputter coated with gold prior to examination. Dynamic rheological properties of the PLA/PBAT blends were assessed using a strain-controlled rheometer (Rheometric Scientific, RDA III). Samples were tested using a parallel-plate geometry ($d = 25$ mm) operated at 180 °C. All the samples were cut from the injection-molded specimen. The sample was loaded between the parallel plates and melted at 180 °C for 3 min. The parallel plates subsequently compressed the sample to 1 mm thick prior to each test. A strain sweep test was initially conducted to determine the linear viscoelastic region of the materials. A dynamic frequency sweep test was subsequently performed to determine the dynamic properties of the blends. The strain and frequency range used during testing were 5% and 0.1−500 rad/s, respectively. Steady-state shear tests at the same temperature were also conducted to investigate the viscosity−shear rate relationship. Shear rates ranging from 0.05 to 500 1/s were employed.

Results and Discussion

Rheological Properties. G' and G'' of the blends with different PBAT loadings are compared in Figures 1 and 2. In general, neat PLA and PBAT have similar G' and G'' values except, at low frequencies, the G' of PBAT is much higher than that of PLA. PLA followed the characteristic terminal behavior fairly well, i.e., $G' \propto \omega^2$ and $G'' \propto \omega$. On the other hand, the G' of PBAT deviated from the terminal behavior markedly ($G' \propto \omega^{1.24}$). Molecular weight distribution strongly affects the shape of the terminal region. Chains of different sizes relax to equilibrium at different times, which "smears out" the typical relaxation behavior of a monosized polymer melt. The relatively broad molecular weight distribution of PBAT (PI = 2.40) likely accounts for the different relaxation behavior.

In Figure 2, the G''s of the blends remain largely unaffected with the variation of PBAT content since the G''s of neat PLA and PBAT are close. The much higher G' of PBAT in Figure

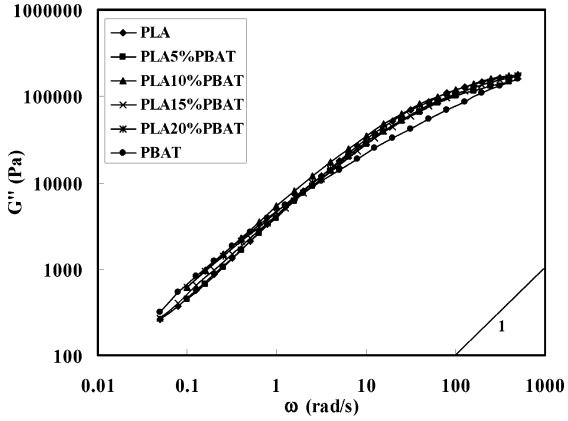

Figure 2. *G″* of PLA/PBAT blends.

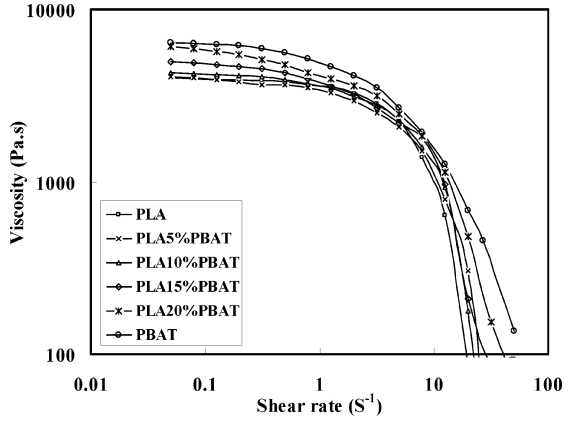

Figure 3. Steady shear viscosities of PLA/PBAT blends.

1 indicates higher elasticity of PBAT than that of PLA at low frequencies. The *G′* of the blends increased with increase in PBAT content. This means that the elasticity of the blend melt increases with PBAT at low frequencies.

PBAT showed higher steady shear viscosities than PLA (Figure 3). The addition of PBAT resulted in the gradual increase in the viscosity of the blends. It also appeared that PLA had a longer Newtonian region than PBAT, and the addition of PBAT reduced the Newtonian region of the blends.

Although rheology data indicate a higher viscosity of PBAT than PLA at 180 °C, the addition of PBAT was found to increase the processability of PLA in extrusion. Barrel temperatures were set to a profile ranging from 150 to 180 °C during extrusion to reduce thermal impact and minimize polymer degradation. PLA (T_m = 154 °C) pellets are rigid and very difficult to compress in a screw flute. During extrusion PLA pellets exist in the first few sections of the barrel due to the low-temperature profile. This led to large resistance to melt flow and thus caused high screw torque and extrusion pressure in the neat PLA extrusion. The melting point of PBAT is much lower (120 °C) compared to that of PLA. It melted from the first section of the barrel and then acted as lubricant to help transfer PLA pellets. As such, the screw torque and extrusion pressure were reduced. In injection molding, due to PBAT's higher viscosity and elasticity, higher injection pressure must be used to fill mold cavities.

Thermal Analysis. DMA results of pristine polymers and blends are shown in Figure 4. Each pristine polymer showed one peak (glass transition). DMA of all the blends revealed a typical two-phase system, showing two glass transitions, one for PBAT at ca. −30 °C and one for PLA at ca. 60 °C. The glass transition temperatures remain unchanged with varying PBAT concentrations, indicating the lack of significant molecular interactions between PLA and PBAT.

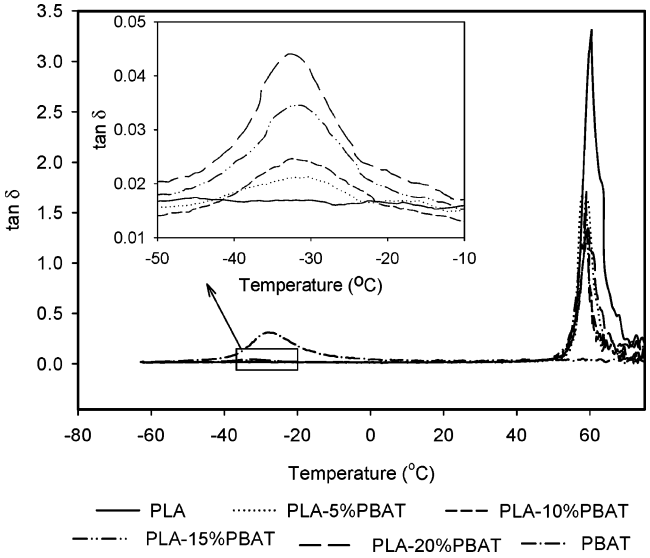

Figure 4. Mechanical loss factor (tan δ) vs temperature for various PLA/PBAT blends. Details of the transition at low temperature, as shown in the box, are enlarged in the inset for clarification.

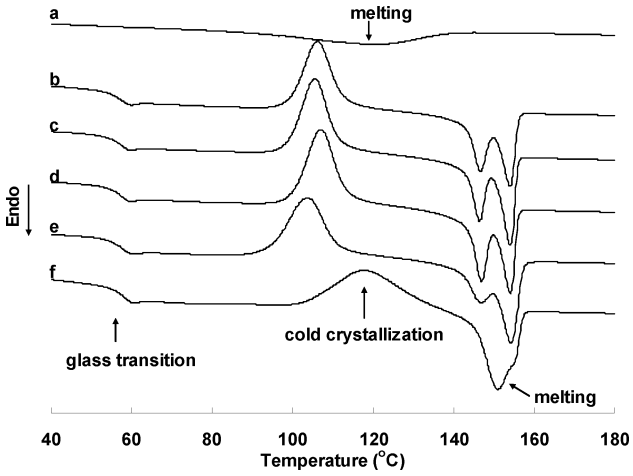

Figure 5. Melting curves of PLA/PBAT blends. Heating rate = 5 °C/min. Data from the second heat. (a) PBAT; (b) 20% PBAT; (c) 15% PBAT; (d) 10% PBAT; (e) 5% PBAT; (f) PLA.

DSC heating curves of PLA, PBAT, and PLA/PBAT blends after crystallizing from melt are shown in Figure 5. Neat PLA displayed a cold crystallization exotherm at 117.8 °C. Comparing curves b−e with f, the incorporation of PBAT decreased cold crystallization temperature by approximate 10 °C and narrowed the peak width, indicating an enhanced crystalline ability of PLA. The very similar ΔH_c and ΔH_m values for each sample (Table 1) indicate that the PLA was primarily amorphous when it was cooled from melt at 30 °C/min. This result suggests that PLA was not able to crystallize within the cooling time frame. Table 1 also shows that ΔH_c and ΔH_m of neat PLA at a heating rate of 10 °C/min are much smaller than those at 5 °C/min, suggesting that neat PLA did not have enough time to complete crystallization at the higher heating rate and displayed low crystallinity. Nevertheless, the recrystallization of the PLA in the blends proceeded to almost the same extent regardless of the scanning rate and PBAT concentration. Therefore, it could be concluded that compared to neat PLA, the addition of PBAT greatly increased the crystallization rate of PLA; and given enough time (e.g., when heating at 5 °C/min), neat PLA and PLA in the blend will crystallize to the same degree. Therefore, adding PBAT did not increase the final crystallinity of the PLA in the blends.

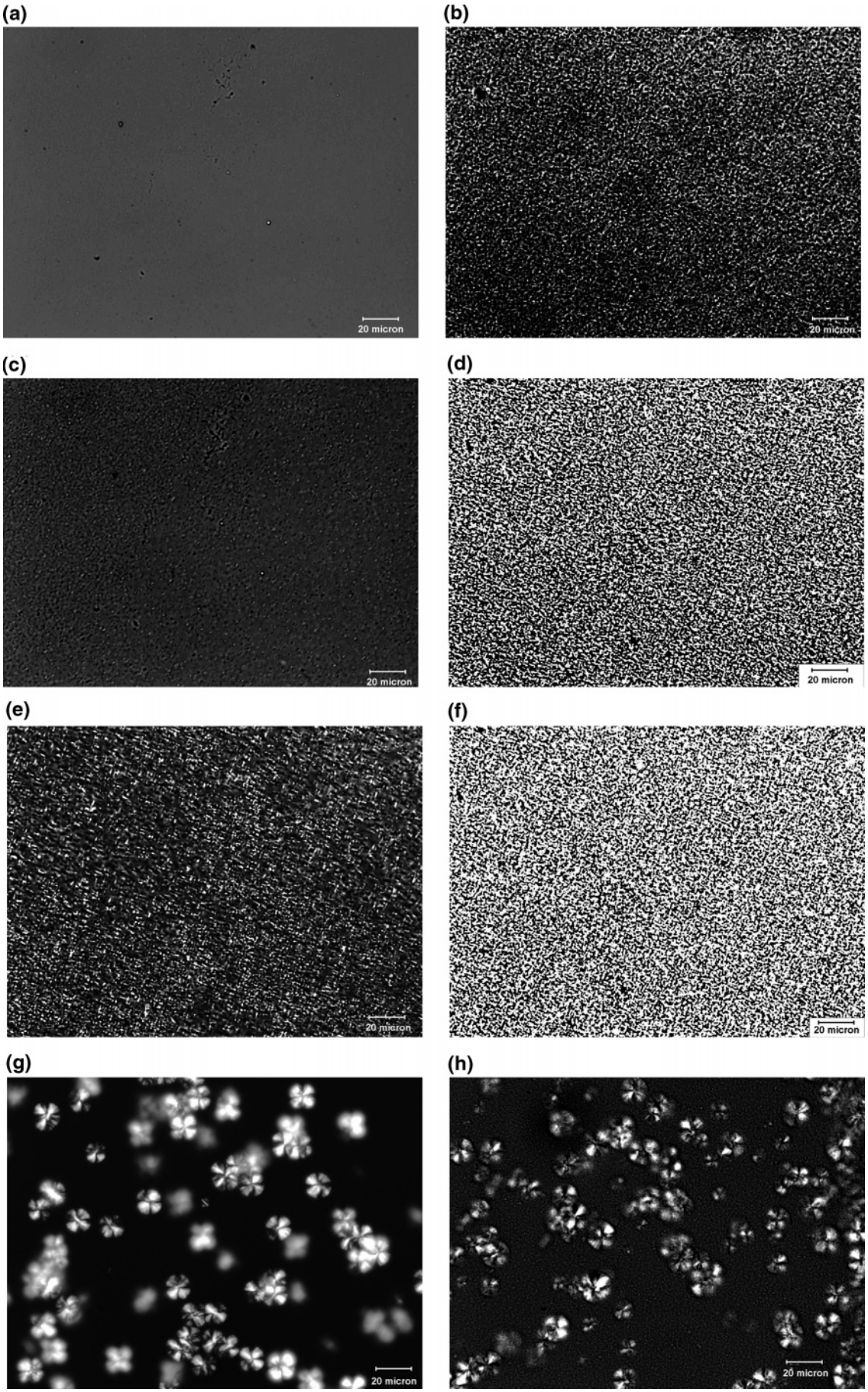

Figure 6. Recrystallization of neat PLA and the PLA−5% PBAT blend during heating. Photos taken under polarized microscope. Heating rate = 10 °C/min. (a) Neat PLA, 100 °C; (b) PLA−5% PBAT, 100 °C; (c) neat PLA, 120 °C; (d) PLA−5% PBAT, 120 °C; (e) neat PLA, 140 °C; (f) PLA−5% PBAT, 140 °C; (g) neat PLA, isothermal at 110 °C for 15 min; (h) PLA−5% PBAT, isothermal at 110 °C for 15 min.

Table 1. T_c, ΔH_c, T_m, and ΔH_m of PLA in Neat Form and Blends at Different Heating Rates[a]

	5 °C/min					10 °C/min				
PBAT content (%)	T_c (°C)[b]	ΔH_c (J/g)[c]	T_m (°C)[b] 1	2	ΔH_m (J/g)[c]	T_c (°C)	ΔH_c (J/g)	T_m (°C) 1	2	ΔH_m (J/g)
0	117.8	23.4	151.1	154.3	23.5	127	9.12		153.3	11.0
5	103.7	25.3	146.9	154.3	26.7	112	24.5	148.8	153.8	24.7
10	106.9	23.7	146.9	154.1	24.0	118	25.2	150.3	153.3	25.3
15	105.4	23.1	146.4	154.1	24.9	116	26.0	149.3	153.8	26.1
20	106.2	24.3	146.7	154.1	24.5	118	24.7	149.3	153.3	25.5
100			120.1		14.9				122.3	15.6

[a] T_c, recrystallization temperature; ΔH_c, enthalpy of crystallization; T_m, melting temperature; ΔH_m, enthalpy of fusion. [b] T_c and T_m are taken at the peak maximum of the crystallization and melting peaks. [c] ΔH_c and ΔH_m are corrected for the content of PLA in the blend.

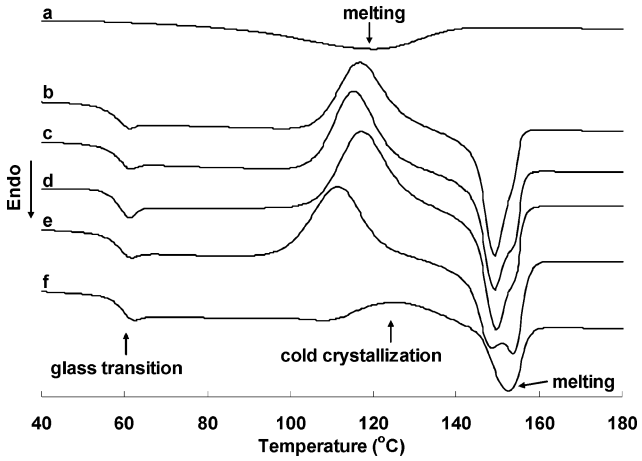

Figure 7. Melting curves of PLA/PBAT blends. Heating rate = 10 °C/min. Data from the second heat. (a) PBAT; (b) 20% PBAT; (c) 15% PBAT; (d) 10% PBAT; (e) 5% PBAT; (f) PLA.

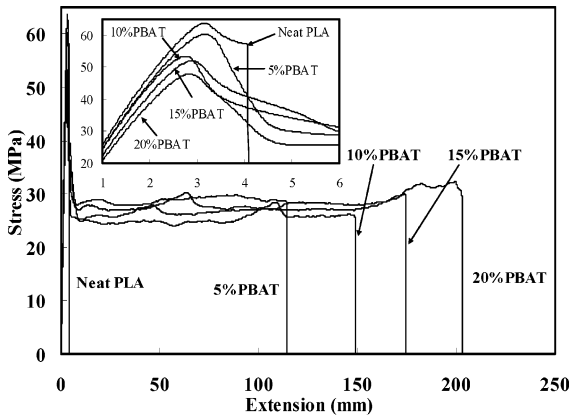

Figure 8. Tensile stress−extension curves of the blends with different PBAT contents. The inset gives details of stress−extension of the blends in the neighborhood of yield points.

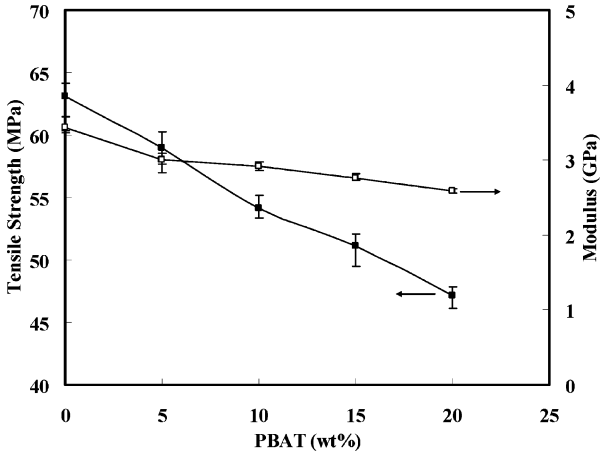

Figure 9. Tensile strength and modulus of blends with different PBAT contents.

The cold crystallization of PLA in neat form and blend with 5% PBAT was further investigated using a polarized optical microscope, and the samples were heated at the same heating rate as in the DSC scan using a Linklam hot stage (Figure 6). Parts g and h of Figure 6 show spherulites of neat PLA and PLA−5% PBAT under polarized microscope. The samples were melted at 180 °C for 2 min and then cooled to 110 °C by 30 °C/min. The photo was taken after 15 min of isothermal treatment at 110 °C. The typical crosslike extinction patterns of spherulites are apparent in the two micrographs. To study cold crystallization, the same temperature ramp profile was used as that in DSC testing. Samples were melted at 180 °C for 2 min and subsequently cooled to 30 °C by 30 °C/min. Then the samples were heated to 180 °C by 10 °C/min. Photos were taken at 100, 120, and 140 °C and are shown in Figure 6a−f. The spherulites in cold crystallization are small and appear in large quantity. The extinction pattern is therefore barely recognizable (Figure 6e). In all these photos, the dark shadows in the extinction pattern merge into the photo background which leaves only the bright parts of the pattern easily visible. It is evident from the figures that the blend started to crystallized at a lower temperature than that of neat PLA. At the same temperature, the number of crystals/crystallinity of PLA−5% PBAT is considerably larger than those of neat PLA. This is consistent with DSC enthalpy measurements.

In the DSC thermogram obtained at 5 °C/min (Figure 5), neat PLA shows a melting peak at 151.1 °C with a shoulder at 154.3 °C. The addition of PBAT clearly separated the melting peak and shoulder of neat PLA into two individual peaks as shown in curves b−e. The peaks at higher temperatures correspond to the shoulder of the neat PLA. The peaks at lower temperatures were approximately 3 °C lower than the peak of neat PLA (Table 1), suggesting the presence of a new crystalline structure induced by PBAT. This structure was in the same form as the high-temperature one but with lower lamellar thickness. This bimodal melting peak was induced during the slow DSC scans when the less perfect crystals had enough time to melt and reorganize into crystals with higher structural perfection and remelt at higher temperature.[36]

When the 10 °C/min heating rate is used, the DSC thermogram is different (Figure 7). The melting shoulder that appeared on neat PLA at 5 °C/min disappeared. Double peaks exhibited on PLA/PBAT blends at 5 °C/min corresponded to a peak and a shoulder (except PLA−5% PBAT, which still exhibited two peaks) at higher temperature at 10 °C/min. The peak and shoulder appeared at closer temperatures at 10 °C/min than the two peaks did at 5 °C/min. These differences could be due to

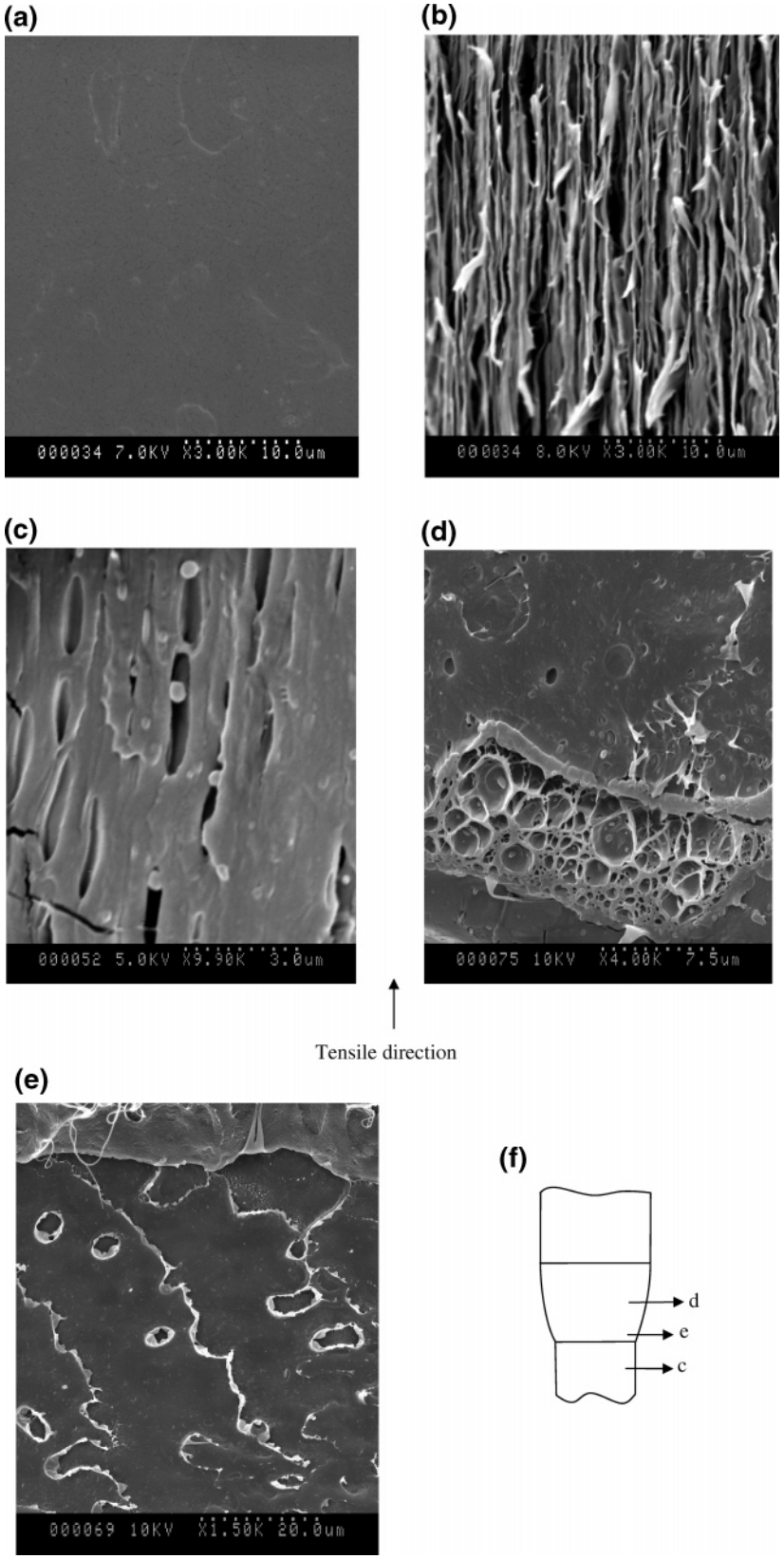

Figure 10. SEM micrographs of PLA and PLA/PBAT blends in the tensile direction. (a and b) were taken ca. 5 mm from the fracture surface. (c−e) were taken at different locations of the necked down region of a PLA−5% PBAT specimen as depicted in (f). (a) Neat PLA; (b) PLA−20% PBAT; (c) PLA−5% PBAT; (d) PLA−5% PBAT; (e) PLA−5% PBAT; (f) approximate locations of parts c, d, and e in the necked down region.

the shorter time for PLA crystals to reorganize to achieve higher perfection at 10 °C/min. They could also be due to the lower resolution of DSC at the higher scanning rate. Like at 5 °C/min, the addition of PBAT enhanced cold crystallization of PLA at 10 °C/min. This was demonstrated by narrower cold crystallization peaks and lower peak temperatures.

Mechanical Properties and Toughening. Fracture behavior of the specimen in the tensile tests changed from brittle fracture

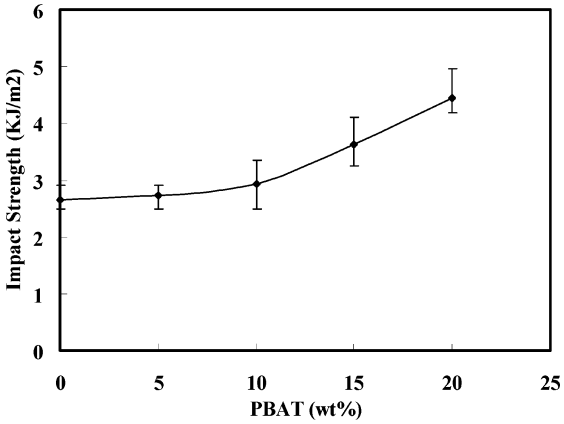

Figure 11. Effect of PBAT concentration in the blends on impact strength.

of the neat PLA to ductile fracture of the blends. This is demonstrated in the tensile stress−extension curves as shown in Figure 8. Neat PLA showed a distinct yield point (maximum load) with subsequent failure by neck instability, and its strain at break was only about 3.7%. On the contrary, all the blends showed distinct yielding and stable neck growth through cold drawing. Surprisingly, it was noticed that even at 5% of PBAT the elongation of the blend was tremendously increased (>200%), and the elongation continuously increased with the increase in PBAT content. Tensile strength and modulus of the PLA/PBAT blends decreased with increasing PBAT content (Figure 9). Tensile strength decreased by 25% from 63 (neat PLA) to 47 MPa (20% PBAT), while modulus decreased by 24% from 3.4 (neat PLA) to 2.6 GPa (20% PBAT).This was expected since PBAT has a lower modulus and tensile strength than PLA.

To study the toughening mechanism of PLA/PBAT blends, the necked down region of the tensile specimen was cryo-fractured longitudinally. SEM micrographs of fractured surfaces are shown in Figure 10. Neat PLA which had no necking in the tensile test showed a smooth longitudinal fracture surface without visible plastic deformation. PLA−20% PBAT had the highest elongation at break, and its matrix experienced tremendous plastic deformation in the stress direction (Figure 10b). For PLA−5% PBAT samples whose elongations are smaller at break, their SEM micrographs (Figure 10c−e) evidently suggest the toughening mechanism. These micrographs were taken at different locations of the necked down region as depicted in Figure 10f, where the stress state varied. Debonding of the round PBAT particles from the PLA matrix under tensile stress is clearly observed. In Figure 10, parts c and d, oval cavities and enclosed round PBAT particles are visible. These cavities were formed during tension when the stress was higher than the

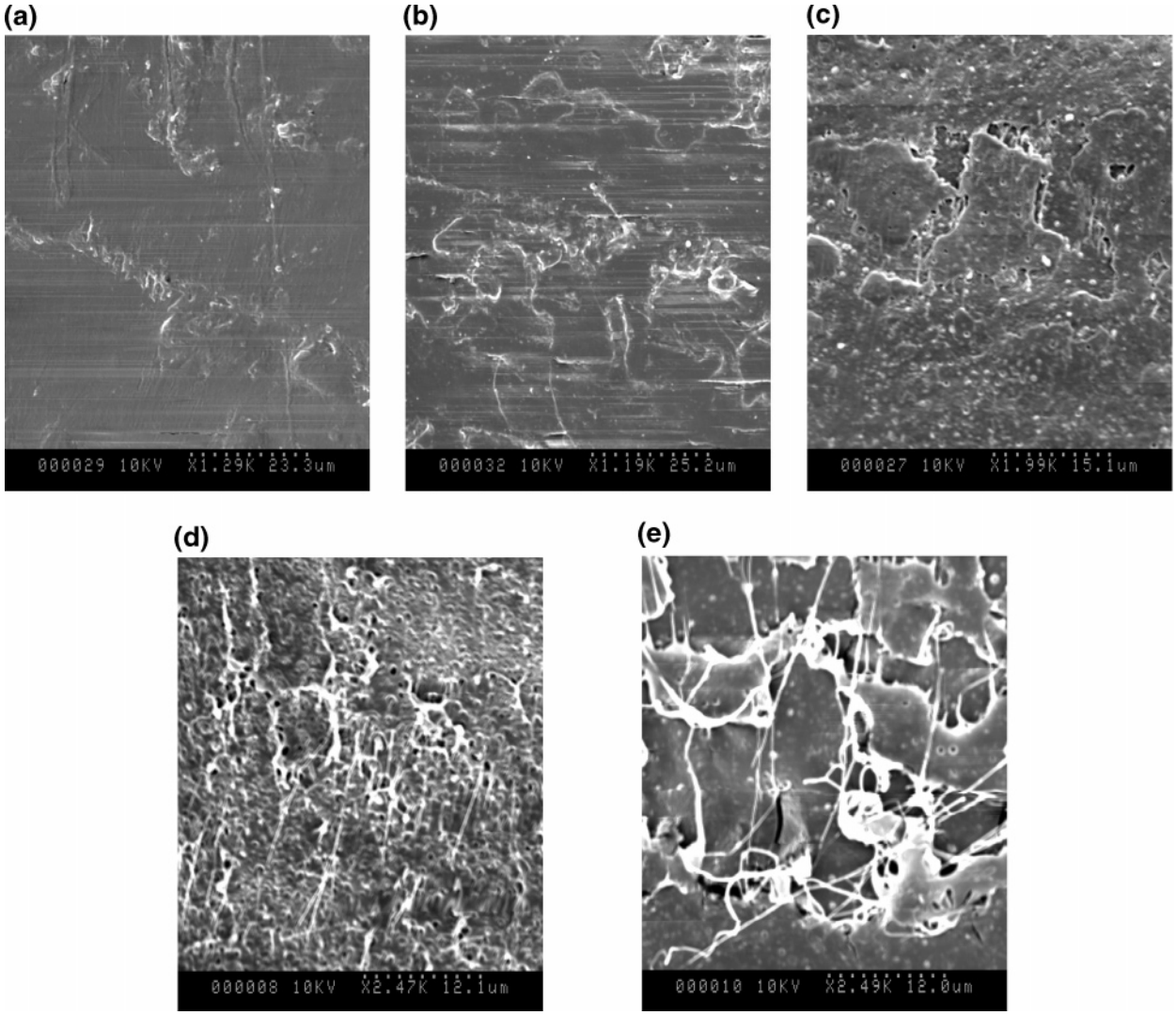

Figure 12. Micrographs of impact-fractured surfaces of blends with different PBAT contents. (a) Neat PLA; (b) 5% PBAT; (c) 10% PBAT; (d) 15% PBAT; (e) 20% PBAT.

bonding strength at the interface between the PLA matrix and PBAT inclusions. PBAT debound from the PLA matrix at the interface, and so cavities arose. These cavities were enlarged in the stress direction along with the deformation of the matrix. Since no stress was applied on PBAT after debonding, PBAT inclusions remained largely undeformed during the course. The white lines in Figure 10e were formed by the coalescence of neighboring cavities. Since PBAT has different elastic properties compared with PLA matrix, its particles act as stress concentrators under tensile stress. The stress concentration gives rise to high triaxial stress in the particles. In rubber-toughened polymer materials, there exist two types of cavitations: either formation of holes within the cores of rubber particles when there is a strong interfacial bonding between the components and relatively weak strength of rubber phase itself or at the interface when the interfacial bonding strength is lower than PBAT strength. Because there was not sufficient interfacial adhesion between PBAT and PLA, instead of cavitation within the PBAT core under the triaxial stress, interfacial debonding took place. The voids caused by debonding altered the stress state in the PLA matrix surrounding the voids, and triaxial tension was locally released and shear yielding was allowed. With the debonding progress, PLA matrix strands between PBAT particles deformed more easily to achieve the shear yielding. This toughening mechanism is in agreement with the findings in other systems. For example, Kim and Michler studied micromechanical deformation processes in various toughened and particle-filled semicrystalline polymers and found that the interfacial adhesion has a great influence in the micromechanical deformation process.[37,38] When there is a interfacial adhesion, the plastic deformation occurs via a single cavitation process inside the modifier particle, whereas when there is not adequat adhesion, the micromechanical deformation process is initiated with debonding.[39,40]

Impact toughness is also increased from 2.6 GPa for neat PLA to 4.4 GPa for PLA−20% PBAT as shown in Figure 11. SEM micrographs of the impact-fractured surfaces show more evidences of ductile fractures as more and longer fibrils can be observed from the surfaces with the increase in PBAT content (Figure 12, where round white particles are the PBAT phase). Crazing, cavitation, shear banding, crack bridging, and shear yielding have been identified as important energy dissipation processes involved in the impact fracture of toughened polymer systems.[39,41−46] In Figure 12d, cavitation caused by debonding can be clearly identified. The large voids in Figure 12e might be formed by the coalescence of neighboring small cavities.

Conclusion

PLA and PBAT were melt blended using a twin screw extruder and pelletized for injection molding. Rheological results revealed that PBAT had higher melt elasticity and viscosity than PLA, and the melt elasticity and viscosity of the blends increased with the concentration of PBAT. In addition to toughening PLA, PBAT increased the processability of PLA in extrusion by acting as a lubricant at low extrusion temperature. SEM micrographs show that PBAT was evenly dispersed in the PLA matrix. DMA and DSC results indicated that the blend is an immiscible two-phase system. The addition of PBAT was found to accelerate the crystallization *rate* of PLA but had little effect on its *final degree of* crystallinity. Like in other blend systems, the semicrystalline PLA experienced extensive cold crystallization, and the PLA was almost totally amorphous in the molded products at the normal processing condition. Even with 5% PBAT, the tensile toughness of the PLA blend was greatly increased without severe loss in tensile strength and modulus. The impact strength of the blend was also significantly improved at 10% or higher of PBAT addition. The stress−extension curve showed the material changed from brittle (PLA) to ductile failure with the addition of PBAT. SEM micrographs revealed that a debonding-initiated shear yielding mechanism was involved in the toughening of the blend.

References and Notes

(1) Sodergard, A.; Stolt, M. *Prog. Polym. Sci.* **2002**, *27*, 1123−1163.
(2) Grijpma, D. W.; Zondervan, G. J.; Pennings, A. J. *Polym. Bull.* **1991**, *25*, 327−333.
(3) Wehrenberg, R. H. *Mater. Eng.* **1981**, *94*, 63−66.
(4) Hiljanen-Vainio, M.; Karjalainen, T.; Seppala, J. V. *J. Appl. Polym. Sci.* **1996**, *59*, 1281−1288.
(5) Hiljanen-Vainio, M.; Orava, P. A.; Seppala, J. V. *J. Biomed. Mater. Res.* **1997**, *34*, 39−46.
(6) Buchholz, B. *J. Mater. Sci.: Mater. Med.* **1993**, *4*, 381−388.
(7) Nakayama, A.; Kawasaki, N.; Arvanitoyannis, I.; Iyoda, J.; Yamamoto, N. *Polymer* **1995**, *36* (6), 1295−1301.
(8) Joziasse, C. A. P.; Grablowitz, H.; Pennings, A. J. *Macromol. Chem. Phys.* **2000**, *201*, 107−112.
(9) Kylma, J.; Seppaela, J. V. *Macromolecules* **1997**, *30* (10), 2876−2882.
(10) Storey, R. F.; Wiggins, J. S.; Puckett, A. D. *J. Polym. Sci., Part A: Polym. Chem.* **1994**, *32* (12), 2345−2363.
(11) Stolt, M.; Hiltunen, K.; Sodergard, A. *Biomacromolecules* **2001**, *2* (4), 1243−1248.
(12) Aslan, S.; Calandrelli, L.; Laurienzo, P.; Malinconico, M.; Migliaresi, C. *J. Mater. Sci.: Mater. Med.* **2000**, *35* (7), 1615−1622.
(13) Hiljanen-Vainio, M.; Varpomaa, P.; Seppala, J.; Tormala, P. *Macromol. Chem. Phys.* **1996**, *197* (4), 1503−1523.
(14) Maglio, G.; Migliozzi, A.; Palumbo, R.; Immirzi, B.; Volpe, M. G. *Macromol. Rapid Commun.* **1999**, *20* (4), 236−238.
(15) Maglio, G.; Malinconico, M.; Migliozzi, A.; Groeninckx, G. *Macromol. Chem. Phys.* **2004**, *205* (7), 946−950.
(16) Meredith, J. C.; Amis, E. J. *Macromol. Chem. Phys.* **2000**, *201* (6), 733−739.
(17) Kim, C.-H.; Cho, K. Y.; Choi, E.-J.; Park, J.-K. *J. Appl. Polym. Sci.* **2000**, *77* (1), 226−231.
(18) Kylma, J.; Hiljanen-Vainio, M.; Seppala, J. *J. Appl. Polym. Sci.* **2000**, *76* (7), 1074−1084.
(19) Kylma, J.; Seppala, J. *J. Appl. Polym. Sci.* **2000**, *79* (8), 1531−1539.
(20) Hiljanen-Vainio, M.; Kylmae, J.; Hiltunen, K.; Seppaelae, J. V. *J. Appl. Polym. Sci.* **1997**, *63* (10), 1335−1343.
(21) de Jong, S. J.; Van Dijk-Wolthuis, W. N. E.; Kettenes-Van den Bosch, J. J.; Hennink, W. E. *Proc. Int. Symp. Controlled Release Bioact. Mater.* **1999**, *26*, 691−692.
(22) de Jong, S. J.; Van Dijk-Wolthuis, W. N. E.; Kettenes-van den Bosch, J. J.; Schuyl, P. J. W.; Hennink, W. E. *Macromolecules* **1998**, *31* (19), 6397−6402.
(23) Tsuji, H.; Ikada, Y. *Macromolecules* **1992**, *25*, 5719−5723.
(24) Tsuji, H.; Ikada, Y. *Polymer* **1999**, *40* (24), 6699−6708.
(25) Tsuji, H.; Hyon, S. H.; Ikada, Y. *Macromolecules* **1991**, *24*, 5657−5662.
(26) Tsuji, H.; Hyon, S. H.; Ikada, Y. *Macromolecules* **1992**, *25*, 2940−2946.
(27) Tsuji, H.; Hyon, S. H.; Ikada, Y. *Macromolecules* **1991**, *24*, 5651−5656.
(28) Wang, Y.; Hillmyer, M. A. *J. Polym. Sci., Part A: Polym. Chem.* **2001**, *39* (16), 2755−2766.
(29) Nakafuku, C.; Sakoda, M. *Polym. J.* **1993**, *25* (9), 909−917.
(30) Malzert, A.; Boury, F.; Saulnier, P.; Benoit, J. P.; Proust, J. E. *Langmuir* **2000**, *16* (4), 1861−1867.
(31) Gajria, A. M.; Davé, V.; Gross, R. A.; McCarthy, S. P. *Polymer* **1996**, *37* (3), 437−444.
(32) Zhang, L.; Goh, S. H.; Lee, S. Y. *Polymer* **1998**, *39* (20), 4841−4847.
(33) Avella, M.; Errico, M. E.; Immirzi, B.; Malinconico, M.; Martuscelli, E.; Paolillo, L.; Falcigno, L. *Angew. Makromol. Chem.* **1997**, *246*, 49−63.
(34) Avella, M.; Errico, M. E.; Immirzi, B.; Malinconico, M.; Falcigno, L.; Paolillo, L. *Macromol. Chem. Phys.* **2000**, *201* (12), 1295−1302.
(35) Witt, U.; Einig, T.; Yamamoto, M.; Kleeberg, I.; Deckwer, W. D.; Muller, R. J. *Chemosphere* **2001**, *44*, 289−299.

(36) Sarasua, J.-R.; Prud'homme, R. E.; Wisniewski, M.; Borgne, A. L.; Spassky, N. *Macromolecules* **1998**, *31*, 3895−3905.
(37) Kim, G. M.; Michler, G. H. *Polymer* **1998**, *39* (23), 5699−5703.
(38) Kim, G. M.; Michler, G. H. *Polymer* **1998**, *39* (23), 5689−5697.
(39) Wu, J. S.; Yee, A. F.; Mai, Y. W. *J. Mater. Sci.* **1994**, *29*, 4510−4522.
(40) Kim, G. M.; Michler, G. H.; Gahleitner, M.; Fiebig, J. *J. Appl. Polym. Sci.* **1996**, *60*, 1391−1403.
(41) Kunz-Douglass, S.; Beaumont, P. W. R.; Ashby, M. F. *J. Mater. Sci.* **1980**, *15*, 1109−1123.
(42) Pearson, R. A.; Yee, A. F. *J. Mater. Sci.* **1991**, *26*, 3828−3844.
(43) Kambour, R. P.; Russell, R. R. *Polymer* **1971**, *12*, 237−246.
(44) Wu, S. *Polymer* **1985**, *26*, 1855−1863.
(45) Bucknall, C. B.; Clayton, D.; Keast, W. E. *J. Mater. Sci.* **1973**, *8*, 514−524.
(46) Yee, A. F.; Li, D.; Li, X. J. *J. Mater. Sci.* **1993**, *28*, 6392−6398.

BM050581Q